JOURNAL OF AGRICULTURAL AND FOOD CHEMISTRY

Article

pubs.acs.org/JAFC

Chemistry of Color Formation during Rooibos Fermentation

Theres Heinrich, Ina Willenberg, and Marcus A. Glomb*

Institute of Chemistry, Food Chemistry, Martin-Luther-University Halle-Wittenberg, Kurt-Mothes-Str. 2, 06120 Halle, Germany

ABSTRACT: Nonenzymatic oxidative degradation of aspalathin, a dihydrochalcone unique to green rooibos (*Aspalathus linearis*), resulted in formation of the characteristic red−brown color of processed rooibos tea. As recently reported, two colorless dimers were formed by oxidative coupling. Incubations of aspalathin showed further distinct signals. Isolation by multilayer countercurrent chromatography (MLCCC) followed by preparative high-performance liquid chromatography (HPLC) led to pure substances. Subsequent analysis by NMR and MS techniques identified a third colorless dimeric compound. In addition for the first time, two colored structures with dibenzofuran skeleton, (*S*)- and (*R*)-3-(7,9-dihydroxy-2,3-dioxo-6-*β*-D-glucopyranosyl-3,4-dihydrodibenzo[*b*,*d*]furan-4*a*(2*H*)-yl) propionic acid, and their corresponding mechanistic precursors were unequivocally established. Color-dilution analysis revealed these compounds as the key chromophores of the incubated aspalathin solutions, ultimately being degraded to unknown, more stable tannin-like structures. Their mechanistic importance to color formation was further underlined by detection of the dibenzofurans also in fermented rooibos tea after trapping with *o*-phenylenediamine as their corresponding quinoxaline derivatives.

KEYWORDS: *Rooibos tea, degradation of dihydrochalcones, aspalathin, quinoxalines, nonenzymatic browning, color dilution analysis*

INTRODUCTION

Aspalathin is a dihydrochalcone and *C*-glycoside unique to rooibos *(Aspalathus linearis)* and represents the major flavonoid of unfermented leaves and stems.[1] During fermentation the amount of aspalathin decreases substantially by almost 98%.[2] The degradation of aspalathin has been shown to contribute significantly to the characteristic red-brown color of processed rooibos tea,[3,4] but none of the resulting colored structures were published so far.

As previously reported, the oxidative degradation of aspalathin is based on a nonenzymatic mechanism in contrast to the processing of black tea *(Camellia sinensis)*.[5] Black tea pigments are initiated by polyphenol oxidase-catalyzed oxidation of the catechins of green tea.[6] The key biochemical event is the formation of quinones that triggers all of the subsequent changes.[7] Quinone formation is determined by catechin's redox potential, relative concentrations, and the oxidative environment. Subsequent reactions such as polymerization result in the formation of bisflavonols, theaflavins, thearubigins, and other oligomers.[8]

In contrast, formation of color during rooibos fermentation is almost solely based on nonenzymatic mechanisms. Two different degradation ways of aspalathin were elucidated so far. The first mechanism describes the initial oxidation of aspalathin to *o*-quinone that converts to isoorientin and orientin via eriodictyol glucopyranosides.[9,10] A second major pathway of aspalathin in the fermentation process is dimerization, which is again initiated by oxidation. The *o*-quinone is attacked nucleophilically by a second aspalathin molecule.[5] However, with absorbance maxima located at 280 and 350 nm, neither eriodictyols, isoorientin, orientin, nor the dimers are colored substances.

The aim of the present work was to elucidate the chemistry behind color formation during the rooibos tea fermentation process including isolation and identification of discrete colored structures in aspalathin model reactions and in fermented rooibos. In addition by means of color dilution analysis, the impact of target compounds on overall color formation was studied in depth.[11,12]

MATERIALS AND METHODS

Chemicals. Ethyl acetate, *n*-butanol, acetone, and diethyl ether were obtained from Roth (Karlsruhe, Germany). Methanol (high-performance liquid chromatography (HPLC) grade) was from Sigma-Aldrich (Steinheim, Germany). Hydrochloric acid was purchased from Fisher Scientific (Schwerte, Germany), formic acid from VWR (Darmstadt, Germany), and heptafluorobutyric acid from Acros Organics (Geel, Belgium). *o*-Phenylenediamine (OPD) and acetonitrile were supplied from Fluka (Taufkirchen, Germany). Diethylenetriaminepentaacetic acid (DTPA) was from Merck (Darmstadt, Germany). Methanol-d_4 was obtained from Chemotrade (Leipzig, Germany).

Extraction of Rooibos Tea. Unfermented and fermented rooibos tea from Biedouw Valley of South Africa was obtained from Mount Everest Tea Company GmbH (Elmshorn, Germany). For isolation of aspalathin, 100 g of unfermented (green) rooibos were extracted with 1 L of acetone/water (7:3, v/v) at 5 °C for 24 h under argon atmosphere and decanted. Acetone was removed under reduced pressure. The residual H_2O phase was successively extracted with diethyl ether, ethyl acetate, and *n*-butanol. The volume was 2 × 200 mL for each solvent. From the ethyl acetate and *n*-butanol extract, solvents were removed under reduced pressure.

Both extracts were chromatographed on a silica gel column (3 cm ×15 cm) using ethyl acetate/methanol (9:1, v/v) as the eluent. Fractions containing aspalathin were combined, and the organic solvent was removed. The residue was further purified using a LiChroprep RP18 column (Merck, Lobar 310-25, 40−63 μm, Darmstadt, Germany) with water/methanol (73:27, v/v) as the eluent and 0.8 mL L^{-1} formic acid added to the solvent. Eluted liquids were collected in fractions of 17.5 mL at a flow rate of 5 mL min^{-1}. After

Received: January 16, 2012
Revised: April 18, 2012
Accepted: April 21, 2012
Published: May 9, 2012

combining aspalathin fractions, solvents were removed under reduced pressure to yield the product as a colorless solid.

Analytical HPLC-DAD-MS. A Jasco (Gross-Umstadt, Germany) quaternary gradient unit PU 2080, with degasser DG 2080-54, autosampler AS 2055, column oven (Jasco Jetstream II), and multiwavelength detector MD 2015 coupled to an Advantec fraction collector CHF122SB (Tokyo, Japan), was used. Alternatively, the detector was coupled to an API 4000 triple quadruple mass spectrometer (Applied Biosystems, Foster City, CA). Chromatographic separations were performed on two different systems. Detection of compounds **1**−**5**, **10**, and **11** as well as color dilution analysis were done on a stainless steel column (Vydac CRT, #218TP54, 250 × 4.0 mm, RP18, 5 μm, Hesperia, CA) using a flow rate of 1.0 mL min^{-1}. The mobile phase used was water (solvent A) and methanol/water (7:3, v/v, solvent B). To both solvents (A and B), 0.6 mL L^{-1} heptafluorobutyric acid (HFBA) was added. In method A, samples were injected at 10% B, and the gradient was then changed to 30% B in 30 min, to 65% B in 40 min, to 100% B in 2 min, and held at 100% B for 8 min. For color dilution analysis, 80 fractions of 1 mL were collected in 80 min.

Chromatographic separations of compounds **6**−**9** were performed on a stainless steel column (Eurospher 100-5 C18, 250 × 4.6 mm) by Knauer (Berlin, Germany) using a flow rate of 1.0 mL min^{-1}. The mobile phase used consisted of water (solvent C) and methanol/water (7:3, v/v, solvent D). To both solvents (C and D), 0.8 mL L^{-1} formic acid was added. In method B, samples were injected at 2% D, held for 10 min, the gradient was then changed to 65% D in 55 min, to 100% D in 2 min, and held at 100% D for 13 min. The column temperature was always 25 °C. The effluent was monitored at 280, 430, and 450 nm.

MS-ionization was achieved using the Turbospray ionization source operated in positive ion mode. Turbospray settings were as follows: curtain gas (N_2) at 40 psi, ion source gas 1 at 50 psi, and ion source gas 2 at 60 psi, with source temperature at 500 °C and ion spray voltage at 4500 V. Mass spectral data on precursor and product ions were collected. Declustering potential, entrance potential, collision energy, and cell exit potential were optimized for each analyte. Mass spectra obtained for **10** and **11**: m/z 539.2 (M + H, 8%), 521.3 (6), 503.3 (7), 485.2 (6), 449.3 (51), 443.3 (27), 419.2 (100), 401.1 (58%).

Multilayer Countercurrent Chromatography. The multilayer countercurrent chromatography (MLCCC) system (Ito, multilayer separator−extractor model, P.C. Inc., Potomac, MD) was equipped with a Waters constant-flow pump (model 6000 A), a Zeiss spectrophotometer PM2D operating at 280 and 430 nm, and a sample injection valve with a 10 mL sample loop. Eluted liquids were collected in fractions of 16 mL with a fraction collector (LKB Ultrorac 7000). Chromatograms were recorded on a plotter (Servogor 200). The multilayer coil was prepared from 1.6 mm inner diameter (i.d.) poly(tetrafluoroethylene) (PTFE) tubing. The total capacity was 240 mL. The MLCCC was run at a revolution speed of 800 rpm and a flow rate of 2 mL min^{-1} in head-to-tail modus.

For preparative isolation of compounds **1**, **2**, and **5**, aspalathin **3** (22 mM) was dissolved in phosphate buffer (0.2 M, pH 7.4) and incubated (37 °C) for 4 h (**1** and **2**) and 6 h (**5**), respectively, in a shaker incubator (New Brunswick Scientific). For isolation of compounds **8** and **9**, aspalathin (4.5 mM) was dissolved and incubated under the same conditions for 24 h. The reactions were stopped by adding hydrochloric acid (1 N (**1**, **2**, and **5**) and 2 N (**8** and **9**)) with 1 mM diethylenetriaminepentaacetic acid (DTPA). Incubated samples were dissolved in the heavy phase and injected into the system after breakthrough of the mobile phase. The solvent system for all separations consisted of ethyl acetate/*n*-butanol/water (3:1:4 (v/v)).

Incubation of Dibenzofurans 8 and 9 and Fermented Rooibos Tea in the Presence of OPD. Isolated dibenzofurans (42 mM) and OPD (50 mM) were dissolved in phosphate-buffered solution (0.1 M, pH 7.4), and the mixture was maintained for 5 h at room temperature under aerated conditions. Ten g of fermented rooibos were extracted with 100 mL of boiled water. The H_2O phase was incubated with an excess of OPD for 5 h at room temperature under aerated conditions.

Preparative HPLC-UV. A Besta HD 2-200 pump (Wilhelmsfeld, Germany) was used at a flow rate of 8 mL min^{-1}. Elution of materials was monitored by an UV detector (Jasco UV-2075, Gross-Umstadt, Germany). Chromatographic separations were performed on a stainless steel column (Vydac CRT, #218TP1022, 250 × 23 mm, RP18, 10 μm, Hesperia, CA). The mobile phase used was solvents A and B, identical to the analytical HPLC-DAD system. From the individual chromatographic fractions, solvents were removed under reduced pressure. After addition of water, solutions were freeze-dried.

Accurate Mass Determination. The high-resolution positive and negative ion electrospray ionization (ESI) mass spectra (HR-MS) were obtained from a Bruker Apex III Fourier transform ion cyclotron resonance (FT-ICR) mass spectrometer (Bruker Daltonics, Billerica, MA) equipped with an Infinity cell, a 7.0 T superconducting magnet (Bruker, Karlsruhe, Germany), a radio frequency (RF)-only hexapole ion guide, and an external electrospray ion source (APOLLO; Agilent, off-axis spray). Nitrogen was used as the drying gas at 150 °C. The samples were dissolved in methanol, and the solutions were introduced continuously via a syringe pump at a flow rate of 120 μL h^{-1}. The data were acquired with 256K data points and zero filled to 1024K by averaging 32 scans.

Ultra-Performance Liquid Chromatography Time-of-Flight Mass Spectrometry. Chromatographic separations were carried out on an Acquity HSS-T3 C18 column (100 × 1 mm i.d., 1.7 μm) (Waters, Milford, MA) maintained at 40 °C using a Waters Acquity ultra-performance liquid chromatography (UPLC) system (Waters). Elution was performed at a flow rate of 150 μL min^{-1} with the following solvent system: (E) 0.1% formic acid−water and (F) 0.1% formic acid−acetonitrile. Samples were injected at 5% F, and held at 5% F for 1 min, the gradient then increased to 95% F in 15 min, and continued at 95% F for 2 min, then changed to 5% F in 0.01 min, and held at 5% F for 1.99 min. Aspalathin **3** (4.5 mM) was dissolved in water and incubated (37 °C) for 10 h. Detection was performed on a Bruker microTOF (time-of-flight) mass spectrometer (Bruker, Rheinstetten, Germany) equipped with an electrospray ionization (ESI) source operating in the positive ion mode from 100 to 1000 m/z with an acquisition time of 0.3 s in centroid mode. The ESI conditions were as follows: capillary voltage 5000 V, desolvation temperature 190 °C, and desolvation gas flow 360 L h^{-1}.

Nuclear Magnetic Resonance Spectroscopy. NMR experiments were performed on a Bruker Avance III 800 NMR spectrometer (Bruker, Rheinstetten, Germany) operating at 800 MHz for ^1H and 200 MHz for ^{13}C. Chemical shifts are given relative to external Me_4Si and were referenced to internal Me_4Si (δ = 0 ppm, ^1H) and internal CD_3OD (δ = 49.0 ppm, ^{13}C).

Incubation of Aspalathin for Color Dilution Analysis. For determination of the impact of compounds **8** and **9** to total color formation, aspalathin **3** (4.5 mM) was dissolved in phosphate-buffered solution (0.2 M, pH 7.4) and incubated at 37 °C for 24 h. The reaction was stopped by adding hydrochloric acid (1 N with 1 mM DTPA).

Color Dilution Analysis. An aliquot (50 μL) of incubated solution was analyzed by HPLC-DAD for determination of color dilution factor (CD factor). One mL fractions with material exhibiting absorption maxima at 430 nm were then stepwise 1:1 diluted with water. The test was carried out in daylight against a white background. Each dilution was visually judged until the color difference between the diluted fraction and two blanks of tap water could just be visually detected using a triangle test. This dilution was defined as the CD factor. The CD factors evaluated by four different panelists in three independent sessions were averaged. For assignment of the total color dilution factor (CD_{total} factor), 50 μL of incubated solution were diluted to 1 mL and treated as described above.

RESULTS AND DISCUSSION

Oxidative degradation of aspalathin constitutes the major process for change of color during rooibos tea fermentation. As

previously described, two colorless dimers **1** and **2** are formed via oxidative coupling in a first step.[5] During further oxidation the color of the tea changes from green to red−brown. Figure 1

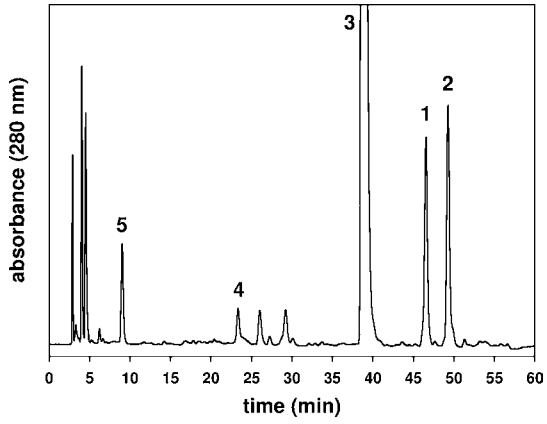

Figure 1. HPLC-DAD chromatogram (method A) of aspalathin after an incubation time of 4 h: dimer **1** (46.6 min); dimer **2** (49.3 min); aspalathin **3** (38.9 min); dimer **4** (23.3 min); dimer **5** (9.0 min). Retention times are given in parentheses. Absorbance maxima for all compounds were λ_{max} = 280 nm.

presents the HPLC-DAD chromatogram of an aerated aspalathin **3** incubation after 4 h. Besides dimers **1** and **2**, two distinct additional signals (**4** and **5**) were formed. However, these colorless substances were completely degraded later. LC-ESI-MS delivered for both signals a pseudomolecular ion of *m*/*z* 923.5 [M + Na^+] and suggested further dimerization of aspalathin **3** based on two oxidation steps in contrast to dimers **1** and **2**. This was confirmed for compound **5** by high-resolution mass spectrometry (HR-MS) (*m*/*z* 923.22248 [M + Na^+] found, *m*/*z* 923.22164 [M + Na^+] calcd for $C_{42}H_{44}O_{22}Na$). Figure 2 shows the yields of dimers **1**, **2**, **4**,

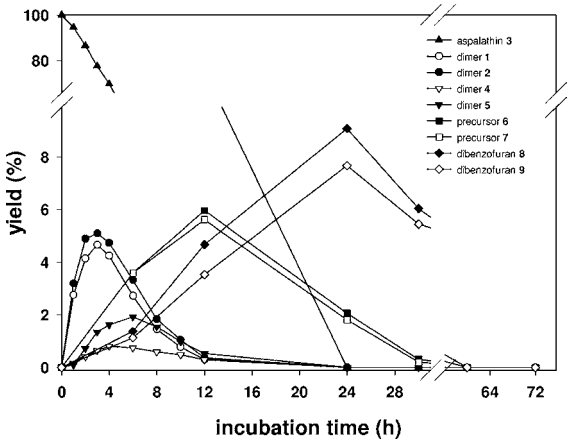

Figure 2. Time-course formation of dimers **1**, **2**, **4**, and **5** and dibenzofurans **8** and **9** with their corresponding precursor structures **6** and **7** during incubation of **3**.

and **5** and aspalathin **3**. Whereas **3** was continuously degraded during the incubation process, **1** and **2** reached maximum concentration after 3 h (4.7% (**1**) and 5.1% (**2**)). **5** was formed later with a maximum at 6 h and at lower concentrations (2%). The very low yields of structure **4** with 0.8% at 4 h in combination with its reactivity did not allow the isolation of enough material for HR-MS measurements nor for further structure elucidation. After 24 h, all compounds were completely degraded to brown end-products with characteristic absorbance maxima at 450 nm. In contrast to **4**, dimer **5** was successfully isolated from a 6 h aspalathin incubation by MLCCC and preparative HPLC. 1D and 2D homonuclear ^1H and heteronuclear $^1H^{13}C$ experiments led to unequivocal structure elucidation of authentic material.

Table 1 provides ^1H and ^{13}C NMR data as well as chemical shift assignments and selected HMBC correlations. Compared

Table 1. ^1H (800 MHz) and ^{13}C NMR (200 MHz) Spectroscopic Data of Dimer 5 (in CD_3OD)[a] and Selected HMBC Correlations

dimer 5

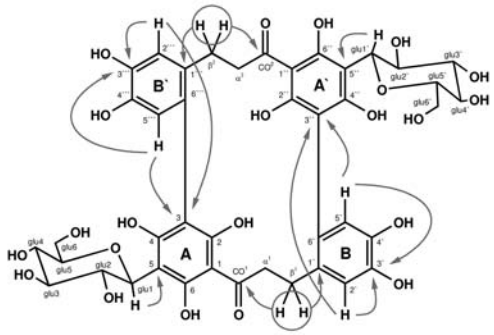

C/H	δ ^1H [ppm]	δ ^{13}C [ppm]
1/1″	-	105.3
2/2″	-	159.6
3/3″	-	109.1
4/4″	-	161.9
5/5″	-	104.2
6/6″	-	163.9
CO^1/CO^2	-	207.2
α^1/α^2	2.81 (ddd[b], 2H, ^2J = 16.6 Hz, ^3J = 12.3 Hz, ^3J = 5.3 Hz) 3.56 (ddd[b], 2H, ^2J = 16.6 Hz, ^3J = 12.3 Hz, ^3J = 3.6 Hz)	45.4
β^1/β^2	2.36 (ddd[b], 2H, ^2J = 13.8 Hz, ^3J = 12.3 Hz, ^3J = 3.6 Hz) 2.66 (ddd[b], 2H, ^2J = 13.8 Hz, ^3J = 12.3 Hz, ^3J = 5.3 Hz)	30.3
1′/1‴	-	135.8
2′/2‴	6.83 (s, 2H)	117.6
3′/3‴	-	147.1
4′/4‴	-	145.2
5′/5‴	6.54 (s, 2H)	120.3
6′/6‴	-	121.9
glu1/glu1′	4.89 (d, 2H, ^3J = 10.3 Hz)	76.3
glu2/glu2′	3.74 (m, 2H)	73.6
glu3/glu3′	3.43 (m, 2H)	79.7
glu4/glu4′	3.41 (m, 2H)	71.2
glu5/glu5′	3.38 (m, 2H)	82.6
glu6/glu6′	3.71 (dd[b], 2H, ^2J = 12.0 Hz, ^3J = 4.4 Hz) 3.84 (dd, 2H, ^2J = 12.0 Hz, ^3J = 1.8 Hz)	62.2

[a] δ, chemical shift; *J*, coupling constant. Hydrogen/carbon assignments were verified by HMBC, HMQC, and ^{13}C-DEPT measurements. [b] Signal was overlapped.

to published NMR data of aspalathin,[9] only two aromatic proton signals were detected, both of them singlets. Because of the correlations to C-3′/C-3‴ and C-4′/C-4‴, both singlets were assigned to the B-/B′-ring. As a result of missing proton multiplicity, the protons are situated in *para*-position, i.e., at positions 2′/2‴ (δ 6.83 ppm) and 5′/5‴ (δ 6.54 ppm), respectively. The presence of ^3J HMBC correlations between C-3 and H-2‴ as well as H-5‴ (likewise C-3″ to H-2′ and H-5′) proved unequivocally the proposed dimeric structure. The molecular mass of 900 amu was in agreement with the double-bonded A- and B-rings of two different aspalathin molecules. Figure 3 depicts the mechanism of formation for this dimer by 2-fold oxidative coupling (pathway A). Initially, aspalathin **3** is autoxidized to an *o*-quinone followed by attack of the A-ring of

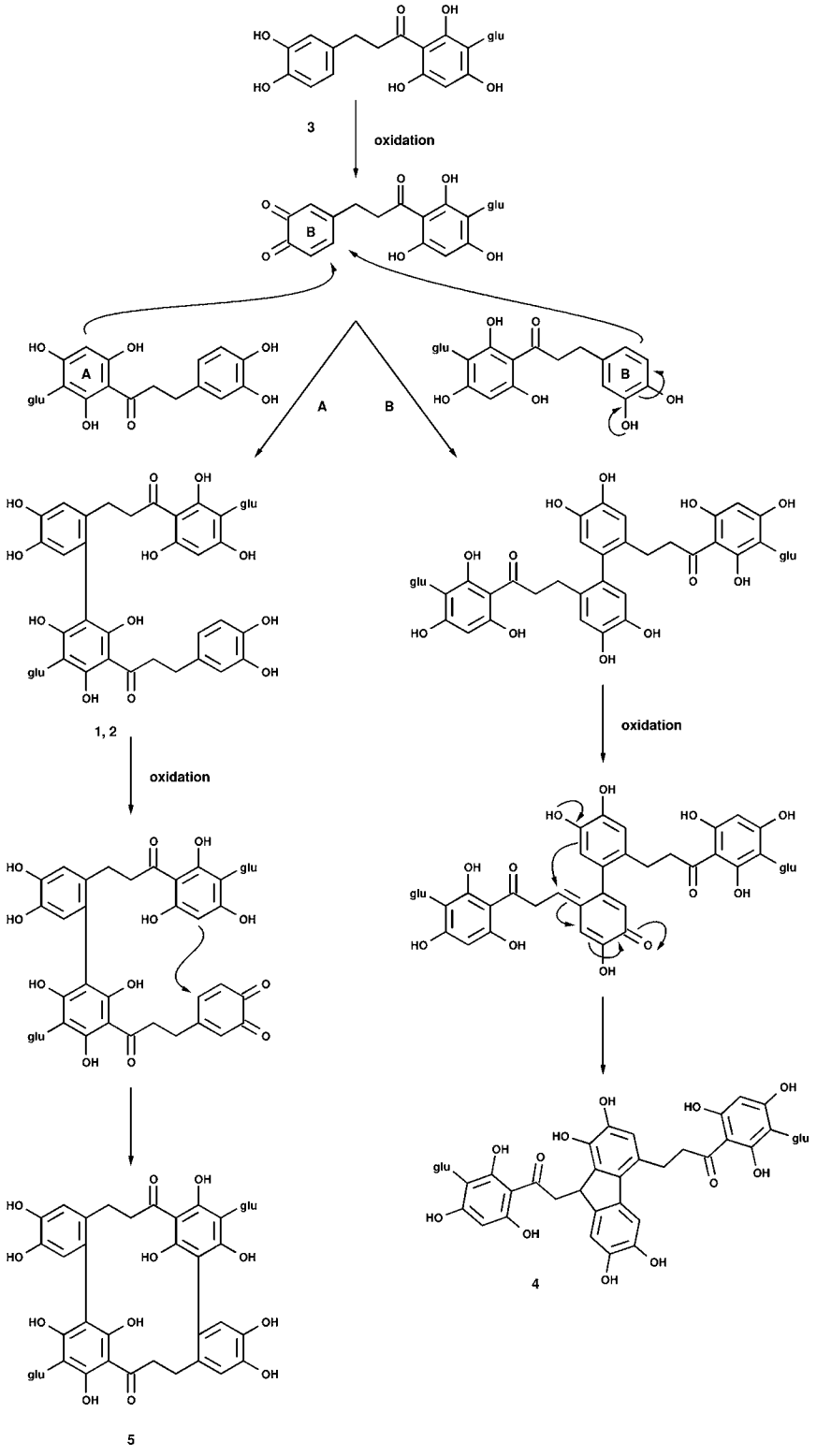

Figure 3. Pathway A: Formation of a new dimer **5** from aspalathin **3** via dimers **1** and **2** by 2-fold oxidative coupling. Pathway B: Postulated pathway of the formation of compound **4** via dimerization of aspalathin **3**. glu = glucose.

a second aspalathin molecule to result in atropisomers **1** and **2**.[5] Further oxidation of the intact B-ring triggers the second nucleophilic attack to form dimer **5**. According to this scheme, dimers **1** and **2** have to be precursor structures of **5**. In support, separate incubation of both isolated **1** and **2** indeed resulted in formation of **5** (data not shown). Furthermore, in contrast to incubations starting from aspalathin, **5** was detected at much higher concentrations and at significantly shorter incubation times (<1 h).

Although it was not possible to isolate structure **4**, the molecular mass of 900 amu again suggested dimerization via a two-step oxidation. Thus, a most likely alternative mechanism is shown in Figure 3 (pathway B). Here the *o*-quinone is nucleophilically attacked by the B-ring of a second aspalathin

Table 2. ^{1}H (800 MHz) and ^{13}C NMR (200 MHz) Spectroscopic Data of Colored Quinoxalines 10 and 11 (in CD_3OD)[a] and Selected HMBC Correlations Observed for Both Quinoxalines

	quinoxaline 10		quinoxaline 11	
	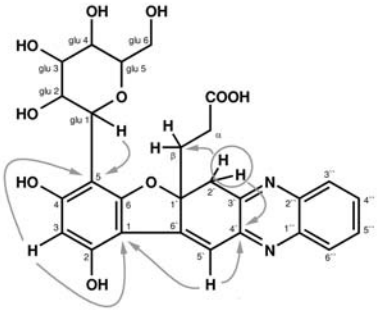			
C/H	δ ^{1}H [ppm]	δ ^{13}C [ppm]	δ ^{1}H [ppm]	δ ^{13}C [ppm]
1	-	108.8	-	109.0
2	-	155.9	-	155.7
3	6.12 (s, 1H)	96.6	6.12 (s, 1H)	96.6
4	-	157.9	-	158.0
5	-	104.7	-	104.7
6	-	156.3	-	156.5
COOH	-	170.3	-	170.1
α	3.07; 3.11; m, 1H	35.2	3.08; 3.11; m, 1H	35.3
β	2.52; 2.54; m, 1H	23.3	2.53; 2.55; m, 1H	23.3
1′	-	127.2	-	127.2
2′	3.47; 3.48; m, 1H	66.8	3.47; 3.49; m, 1H	66.9
3′	-	142.2	-	142.2
4′	-	144.4	-	144.4
5′	7.96 (s, 1H)	131.9	7.96 (s, 1H)	131.9
6′	-	149.8	-	149.9
1″	-	143.8	-	144.2
2″	-	143.6	-	143.6
3″	8.11 (m, 1H)	127.4	8.10 (m, 1H)	127.2
4″	8.22 (m, 1H)	129.8	8.22 (m, 1H)	129.9
5″	8.20 (m, 1H)	129.8	8.21 (m, 1H)	129.9
6″	7.89 (m, 1H)	131.4	7.89 (m, 1H)	131.4
glu1	4.93 (d, 1H, ^{3}J = 9.8 Hz)	77.4	4.92 (d, 1H, ^{3}J = 9.8 Hz)	77.5
glu2	3.79 (m, 1H)	74.6	3.79 (m, 1H)	74.1
glu3	3.49 (m, 1H)	79.5	3.48 (m, 1H)	79.7
glu4	3.48 (m, 1H)	71.2	3.48 (m, 1H)	71.7
glu5	3.38 (m, 1H)	82.4	3.41 (m, 1H)	82.5
glu6	3.74 (dd, 1H, ^{2}J = 12.1 Hz, ^{3}J = 4.8 Hz) 3.84 (dd, 1H, ^{2}J = 12.1 Hz, ^{3}J = 2.2 Hz)	62.1	3.74 (dd, 1H, ^{2}J = 12.1 Hz, ^{3}J = 4.7 Hz) 3.85 (dd, 1H, ^{2}J = 12.1 Hz, ^{3}J = 2.2 Hz)	62.1

[a] δ, chemical shift; J, coupling constant. Hydrogen/carbon assignments were verified by HMBC, HMQC, and ^{13}C-DEPT measurements.

molecule. After rearomatization and oxidation of the second B-ring, the dimer rearranges to a quinone methide.[10] A second nucleophilic attack then leads to putative dimer **4** stabilized by a five-membered ring system.

Parallel to the formation of a red−brown color and to the degradation of aspalathin and the dimers **1**, **2**, **4**, and **5**, other structures with distinct UV and VIS absorbance maxima evolved (Figure 2): **6** (t_R = 18.7 min, λ_{max} = 280 nm), **7** (t_R = 21.6 min, λ_{max} = 280 nm), **8** (t_R = 32.1 min, λ_{max} = 430 nm), and **9** (t_R = 36.5 min, λ_{max} = 430 nm) (method A). HR-MS for **6** and **7** (**6**, m/z 469.1341 [M + H$^+$] found; **7**, m/z 469.1340 [M + H$^+$] found, m/z 469.13405 calcd for $C_{21}H_{25}O_{12}$) and also for **8** and **9** (**8**, m/z 465.10329 [M − H$^-$] found; **9**, m/z 465.10321 [M − H$^-$] found, m/z 465.10275 [M − H$^-$] calcd for $C_{21}H_{21}O_{12}$) revealed two pairs of compounds with identical molecular mass. As HPLC-MS^2 experiments resulted in identical fragmentation patterns for each pair, this suggested isomeric structures.

In an attempt to isolate native **6**, **7**, **8**, and **9** for structure elucidation, all compounds were degraded during workup. However, it was possible to stabilize **8** and **9** by reaction with *o*-phenylenediamine (OPD) as their corresponding quinoxalines **10** (t_R = 40.9 min, λ_{max} = 380 nm) and **11** (t_R = 43.0 min, λ_{max} = 380 nm) (method B). The structure of the isolated quinoxalines was unequivocally established by absorbance maxima at 380 nm, HR-MS (**10**, m/z 539.16604 [M + H$^+$] found; **11**, m/z 539.16612 [M + H$^+$] found, m/z 539.16602 calcd for $C_{27}H_{27}N_2O_{10}$) and 1D and 2D NMR spectroscopic experiments (Table 2). NMR data was virtually identical for **10** and **11**. Four aromatic proton signals resemble in chemical shift and multiplet pattern characteristic for quinoxaline structures.[13] Furthermore, two additional aromatic proton singlets were assigned. Short-range and long-range ^{1}H ^{13}C correlations obtained from heteronuclear single-quantum correlation (HSQC) and heteronuclear multiple bonding correlation (HMBC) spectra, respectively, as well as from published data on aspalathin, clearly verified the singlet H-3 at δ 6.12 ppm belonging to the A-ring.[9] The second singlet at δ 7.96 ppm was attributed to H-5′ because it showed ^{3}J HMBC correlation to C-1 and thus proved unambiguous connection of A- and B-ring via a *O*-heterocyclic five-membered ring system. Moreover, ^{1}H spectra showed signals for three methylene groups besides the

dx.doi.org/10.1021/jf300170j | J. Agric. Food Chem. 2012, 60, 5221−5228

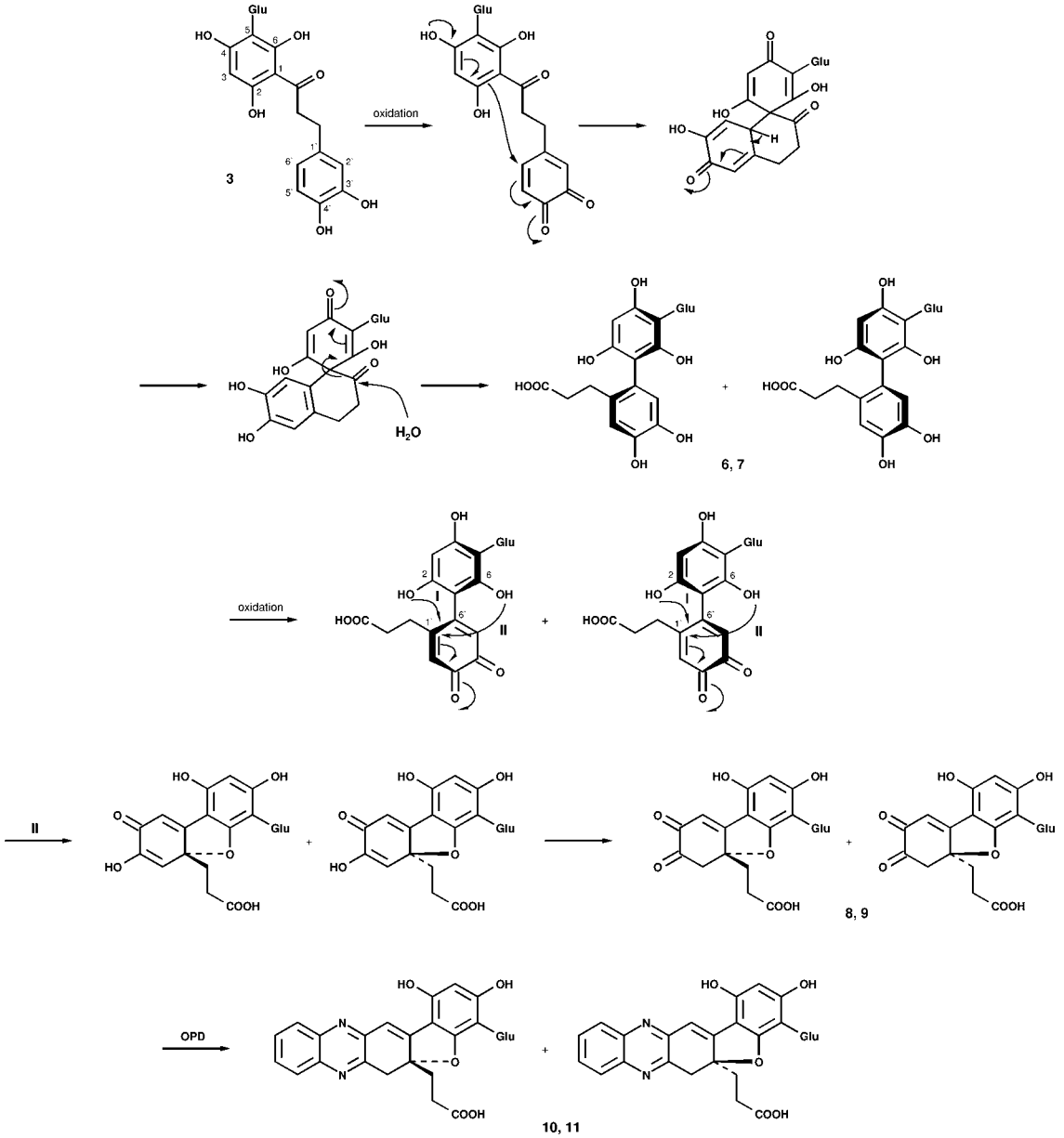

Figure 4. Dibenzofurans **8** and **9** are formed from aspalathin **3** by oxidation via atropisomeric precursors **6** and **7**. glu = glucose.

one of the sugar residue. Two groups at δ 3.10 ppm and δ 2.53 ppm offered vicinal protons and were identified as α and β with the help of 2D ^{1}H COSY. Because of the HMBC correlations to C-4′ and C-6′, the third methylene group H-2′ at δ 3.47 ppm belongs to the former B-ring. The lack of proton multiplicity with singlet H-5′ supports arrangement in *para*-position.

In addition to the quinoxaline NMR data, linkage of sugar moiety at position C-5 was confirmed by HPLC-MS^2 experiments of the native structures **8** and **9**. Li et al. described a reproducible difference between 6-*C*- and 8-*C*-glycosyl flavonoids by comparing the ratios of peak intensity from the mass spectra at selected collision energies.[14] This differentiation was approved by Kazuno et al. and is based mainly on the intensity ratio $[M + H - 150]^+/[M + H - 120]^+$ ion at 30 eV and $[M + H - 120]^+$ at 15/30 eV.[15] Herein, the experiments of structures **8** and **9** resembled typical ratios of 8-*C*-glycosyl flavonoids (ratios for **8**, 0.34 and 0.13; for **9**, 0.70 and 0.35) and thus clearly assigned the sugar residue to C-5.

On the basis of the structure and with regard to the so far known oxidative degradation chemistry of aspalathin, the following mechanism for formation of **8** and **9** is suggested (Figure 4). Reaction starts with oxidation of aspalathin **3** to its *o*-quinone. In an intramolecular Michael-type addition, C-1 of A-ring nucleophilic attacks C-6′ of the *o*-quinone B-ring to result in a new spiro-type six-membered ring. After rearomatization, hydration catalyzes β-dicarbonyl fragmentation to result in the two highly reactive intermediates **6** and **7** with biphenyl structures and propionic acid substituents established by mass spectrometry above. Interestingly, no chiral center is generated during this process. Still both structures showed distinctly different chromatographic behavior. A plausible explanation is that the restricted free rotation due to the three substituents in *ortho*-position to the biaryl axis C-1C-6′ and the voluminous glucose moiety causes atropisomerism.[5] Further oxidation of the former B-ring is then followed by intramolecular ring-closure. As this can be theoretically realized by nucleophilic attack either of the hydroxyl function from C-2

dx.doi.org/10.1021/jf300170j | J. Agric. Food Chem. 2012, 60, 5221−5228

(I) or C-6 (II) at C-1′, keto enol tautomerism leads to two sets of colored diastereoisomers with a dibenzofuran skeleton. However, stabilization by reaction with OPD led only to one pair of quinoxalines **10** and **11**. This unequivocally proves that the nucleophilic attack of strictly OH-6 at C-1′ leads to formation of the identified colored compounds **8** and **9**.

Studies on formation of matlaline from coatline B, a dihydrochalcone of the Mexican medicinal wood *Eysenhardtia polystachya*, substantiate our proposed mechanisms initiated by spontaneous oxidation of dihydrochalcones with a B-ring situated catechol moiety.[16] Interestingly, Le Guernevé et al. described a similar dibenzofuran chromophore from the degradation of phloridzin found in apples.[17] In contrast to aspalathin, phloridzin is an *O*-glucosidic dihydrochalcone and, most importantly, has only one hydroxyl group at the B-ring. In this case the browning is only initiated in the presence of a polyphenol oxidase to give 3-OH-phloridzin, i.e., a catechol moiety at the B-ring. This again clearly depicts the exclusive importance of nonenzymatic aspalathin oxidation chemistry during rooibos fermentation.

Figure 2 shows the yields of **8** and **9** in relation to formation of **6** and **7** during degradation of **3**. As it was not possible to isolate nor to stabilize **6** and **7**, the yields of these two compounds were estimated based on the extinction coefficient of aspalathin. Precursor structures reached their maximum concentration after 12 h in the ratio 58:42 for atropisomer **6**:**7** and were totally degraded after 36 h. On the other hand, the colored products showed the highest yields after 24 h in the ratio 53:47 for dibenzofuran **8**:**9**. The pattern of formation thus proves the postulated reaction pathway as the precursors reached their maximum before the colored products. However, structures **8** and **9** with their characteristic absorbance maximum at 430 nm were also reactive intermediates. After 60 h they were totally degraded while the color of the model incubations changed from yellow to dark orange. Obviously, the breakdown of the dibenzofurans gives rise to high-molecular tannin-like structures during the late stages of aspalathin oxidation, as no further discrete signals for colored compounds were detected in HPLC-DAD.

To determine the contribution of dibenzofurans **8** and **9** to the overall color of the incubated aspalathin solution, color dilution analysis was performed (Figure 5).[18,19] Dilution factors

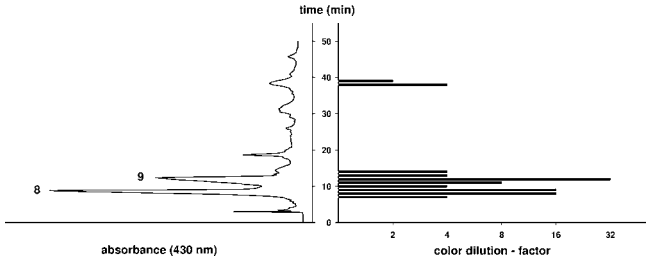

Figure 5. HPLC-DAD chromatogram (λ= 430 nm; left side; method A) and color-dilution chromatogram (right side) of the aspalathin incubation solution after 24 h.

were analyzed at the moment of highest concentration of both compounds and resulted in 15 and 18%, respectively, of the total color (CD_{total} factor = 256). As expected from the reactivity of compounds **8** and **9** as described above, they could not be detected in fermented rooibos tea infusions in their native form. Nevertheless, fermented rooibos infused in the presence of OPD indeed delivered traces of quinoxalines **10** and **11**. The stable derivatives were unequivocally detected in HPLC-DAD and HPLC-MS chromatograms. The mass spectra obtained from the infusions were virtually identical to the authentic reference material.

In summary, we succeeded in elucidation of a novel aspalathin dimer formed by oxidative coupling. In addition, we elucidated for the first time low-molecular colored structures in fermented rooibos with a dibenzofuran skeleton. Color-dilution analysis revealed the major importance of these compounds as key chromophores in the incubated solutions. The dibenzofurans were formed during nonenzymatic oxidative degradation of aspalathin and provide an important step forward to understand the chemistry of color formation during rooibos tea fermentation.

AUTHOR INFORMATION

Corresponding Author

*E-mail: marcus.glomb@chemie.uni-halle.de. Fax: +49-345-5527341.

Notes

The authors declare no competing financial interest.

ACKNOWLEDGMENTS

We thank M. Kovermann from the Institute of Physics, Biophysics Research Group, Halle (Germany), for recording NMR spectra. We are also grateful to J. Schmidt and S. Schmidt from the Leibniz Institute of Plant Biochemistry, Halle (Germany), for performing accurate mass analysis and UPLC/TOF-MS experiments, respectively.

REFERENCES

(1) Baranska, M.; Schulz, H.; Joubert, E.; Manley, M. In situ flavonoid analysis by FT-Raman spectroscopy: Identification, distribution, and quantification of aspalathin in green rooibos (*Aspalathus linearis*). *Anal. Chem.* **2006**, *78*, 7716−7721.

(2) Schulz, H.; Joubert, E.; Schütze, W. Quantification of quality parameters for reliable evaluation of green rooibos (*Aspalathus linearis*). *Eur. Food Res. Technol.* **2003**, *216*, 539−543.

(3) Bramati, L.; Aquilano, F.; Pietta, P. Unfermented rooibos tea: Quantitative characterization of flavonoids by HPLC-UV and determination of the total antioxidant activity. *J. Agric. Food Chem.* **2003**, *51*, 7472−7474.

(4) Joubert, E. HPLC quantification of the dihydrochalcones, aspalathin and nothofagin in rooibos tea (*Aspalathus linearis*) as affected by processing. *Food Chem.* **1996**, *55*, 403−411.

(5) Krafczyk, N.; Heinrich, T.; Porzel, A.; Glomb, M. A. Oxidation of the dihydrochalcone aspalathin leads to dimerization. *J. Agric. Food Chem.* **2009**, *57*, 6838−6843.

(6) Bailey, R. G.; Nursten, H. E.; McDowell, I. The chemical oxidation of catechins and other phenolics: A study of the formation of black tea pigments. *J. Sci. Food Agric.* **1993**, *63*, 455−464.

(7) Graham, H. N. The polyphenols of tea−Biochemistry and significance−A review. *Bull. Liaison−Groupe Polyphenols* **1992**, *16*, 32−43.

(8) Graham, H. N. Green tea composition, consumption, and polyphenol chemistry. *Prev. Med.* **1992**, *21*, 334−350.

(9) Krafczyk, N.; Glomb, M. A. Characterization of phenolic compounds in rooibos tea. *J. Agric. Food Chem.* **2008**, *56*, 3368−3376.

(10) Marais, C.; van Rensburg, W. J.; Ferreira, D.; Steenkamp, J. A. (*S*)- and (*R*)-Eriodictyol-*C*-*β*-D-glucopyranoside, novel keys to the fermentation of Rooibos (*Aspalathus linearis*). *Phytochemistry* **2000**, *55*, 43−49.

(11) Hofmann, T. Characterization of the most intense coloured compounds from Maillard reactions of pentoses by application of colour dilution analysis. *Carbohydr. Res.* **1998**, *313*, 203−213.

(12) Degenhardt, A.; Hofmann, S.; Knapp, H.; Winterhalter, P. Preparative isolation of anthocyanins by high-speed countercurrent chromatography and application of the color activity concept to red wine. *J. Agric. Food Chem.* **2000**, *48*, 5812−5818.
(13) Bravo, A.; Herrera, J. C.; Scherer, E.; Ju-Nam, Y.; Rübsam, H.; Madrid, J.; Zufall, C.; Rangel-Aldao, R. Formation of α-dicarbonyl compounds in beer during storage of Pilsner. *J. Agric. Food Chem.* **2008**, *56*, 4134−4144.
(14) Li, Q. M.; Van den Heuvel, H.; Dillen, L.; Claeys, M. Differentiation of 6-*C*- and 8-*C*-glycosidic flavonoids by positive ion fast atom bombardment and tandem mass spectrometry. *Biol. Mass Spectrom.* **1992**, *21*, 213−221.
(15) Kazuno, S.; Yanagida, M.; Shindo, N.; Murayama, K. Mass spectrometric identification and quantification of glycosyl flavonoide, including dihydrochalcones with neutral loss scan mode. *Anal. Biochem.* **2005**, *347*, 182−192.
(16) Acuna, A. U.; Amat-Guerri, F.; Morcillo, P.; Liras, M.; Rodriguez, B. Structure and formation of the fluorescent compound of *Lignum nephriticum*. *Org. Lett.* **2009**, *11*, 3020−3023.
(17) Le Guernevé, C.; Sanoner, P.; Drilleau, J.-F.; Guyot, S. New compounds obtained by enzymatic oxidation of phloridzin. *Tetrahedron Lett.* **2004**, *45*, 6673−6677.
(18) Frank, O.; Hofmann, T. Characterization of key chromophores formed by nonenzymatic browning of hexoses and L-alanine by using the color activity concept. *J. Agric. Food Chem.* **2000**, *48*, 6303−6311.
(19) Frank, O.; Jezussek, M.; Hofmann, T. Characterisation of novel 1*H*,4*H*-quinolizinium-7-olate chromophores by application of colour dilution analysis and high-speed countercurrent chromatography on thermally browned pentose/L-alanine solutions. *Eur. Food Res. Technol.* **2001**, *213*, 1−7.